Behaviours of Internal Stress and Effective Stress in Fatigue Process

Masaru MATSUDA

The Graduate School of Science and Technology, Kobe University

Rokkodai, Nada, Kobe, 657, JAPAN

Takashi KINUGAWA

The Department of Production Engineering, Kobe University

Rokkodai, Nada, Kobe, 657, JAPAN

Yasushi IKAI

The Department of Production Engineering, Kobe University

Rokkodai, Nada, Kobe, 657, JAPAN

ABSTRACT

In this study, the concept of internal stress and effective stress is introduced into fatigue analysis, followed by a presentation of their measurement. Applied stress is separated into two parts: internal stress and effective stress. Some experimental results are shown and discussed from this viewpoint, and the usefulness of this concept is examined.

The main results obtained are:

(1) A material shows increasing "fatigue resistivity" by stress cycling, which can be monitored in terms of internal stress.

(2) Fatigue damage is accumulated on a surface in the form of surface roughness of the material by alternate plastic strain.

(3) The increment of fatigue damage can be monitored in terms of effective stress, which reflects stress history.

(4) The mechanism of fatigue limit is discussed on the basis of the behaviour of internal stress and effective stress.

(5) A new cumulative damage model is proposed and discussed.

(6) The applied stress fluctuation is aggressive to the material.

Keywords: Internal stress, Effective stress, fatigue limit, Cumulative damage criterion, Transient behaviour.

1. Introduction

Several attempts have been made to elucidate the fatigue limit[1-4]; however, a proper explanation has not been given yet. Moreover, a fatigue damage evaluation on the basis of applied stress often gives incorrect results; in contrast, one based upon plastic strain amplitude gives a better estimation of the fatigue damage. In this regard. a close examination of transient behaviour of the stress-strain relation is necessary. The concept of internal stress and effective stress is introduced in this report into the field of fatigue analysis.

Some experimental results of carbon-steel fatigue tests are shown and discussed from this viewpoint, and the usefulness of this concept is examined.

2. Theory

Applied stress is separated into internal stress and effective stress. This concept has already

been used by Orowan[5] in the early days of dislocation theory, and in particular in studies of high-temperature deformation. Some research work has already been carried out from this point of view in the field of fatigue study. The origin of internal stress and effective stress will be discussed in Appendix A.

2.1 Measurement of internal stresses

Among more than ten methods for measuring the internal stress[6-8], we have chosen the "strain-transient dip test"[9].

At a certain stage of stress cycling, the applied stress is abruptly shifted and held for 20 seconds at a level, in order to find, by trial and error, the stress level where no relaxation strain ε_r is observed, as illustrated in Fig.1. This stress level where $\varepsilon_r=0$ is defined as internal stress, an average value for all moving dislocations. This stress level may show a range, i.e. elastic range, on such a material as steel (See Fig.2). In this case the highest level of the elastic range is defined as internal stress. Effective stress is defined as the difference between applied stress and internal stress.

2.2 Measuring system

In this study, a measuring system was built as shown in Fig.3. A hydraulic fatigue testing machine was controlled by a D-A converted control signal from a personal computer. On the other hand, a signal from

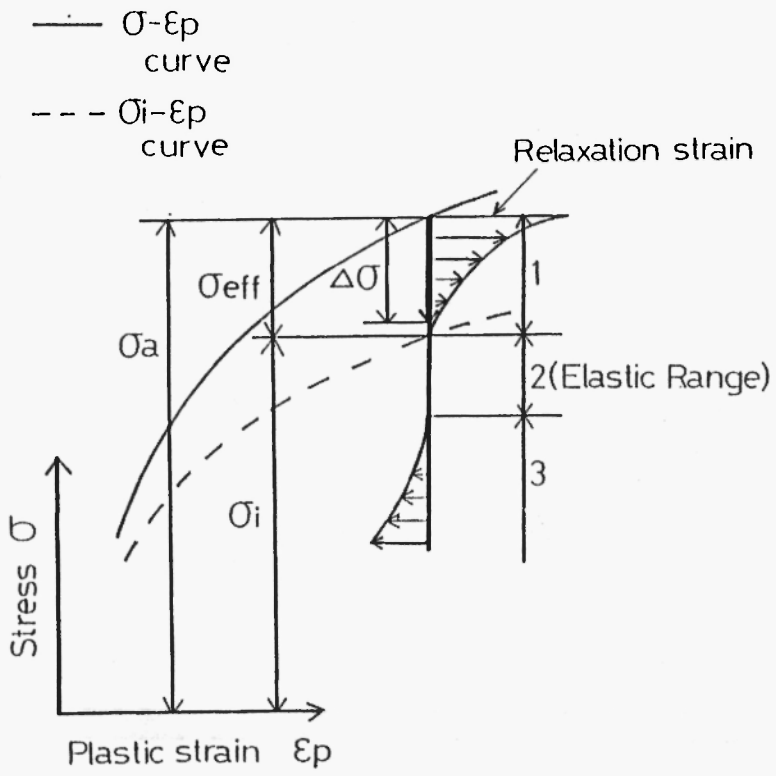

Fig.1 Change in relaxation strain(ε_r) in strain-transient dip test

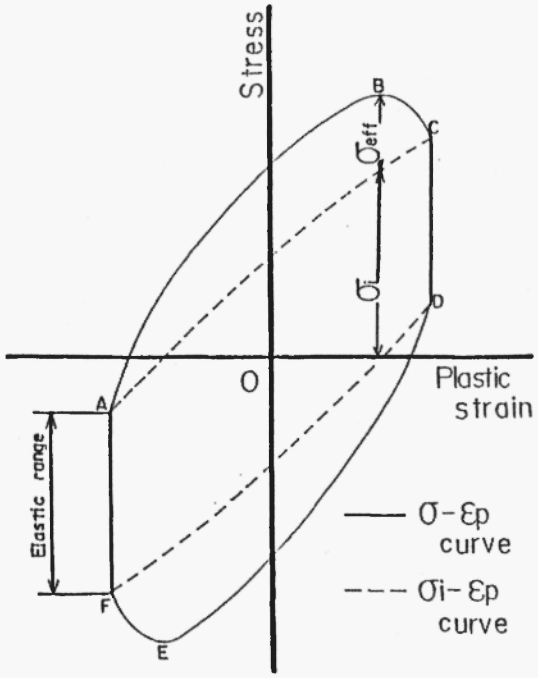

Fig.2 Example of relation among stresses (σ_a and σ_i) and plastic strain (ε_p).

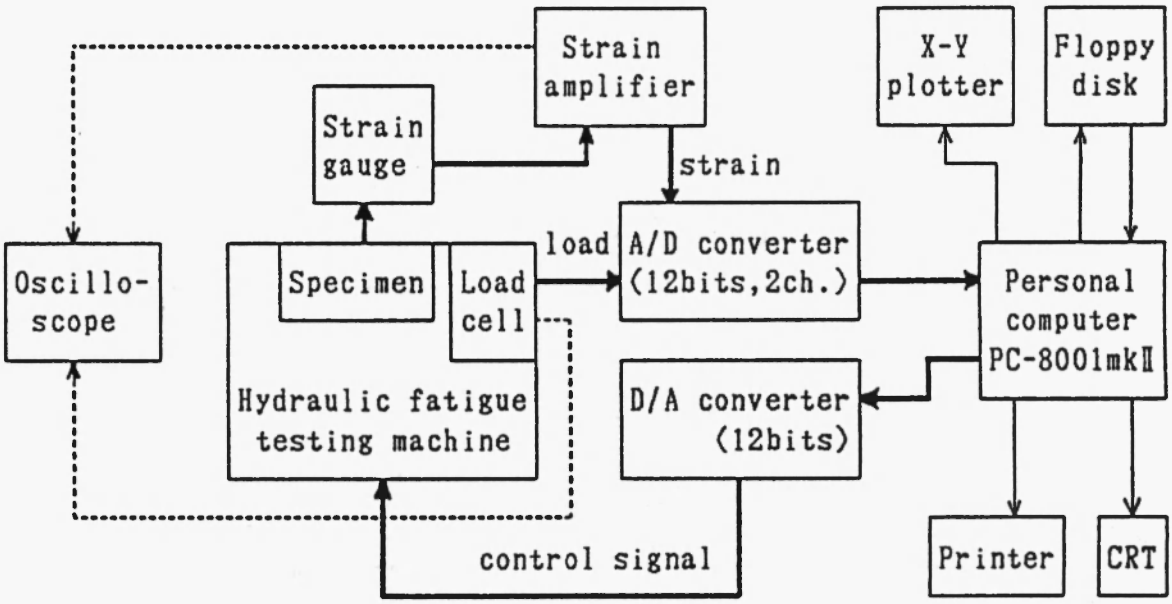

Fig.3 The system of test equipment

the load cell of the machine and also a signal from the strain gauge attached to the specimen were A-D converted and inputted to the computer for control and measurement. The hydraulic testing machine has the ability to hold a stress level with less than 0.30MPa fluctuation in 60 seconds, and this enables us to evaluate internal stress level with a standard deviation less than 3.2MPa.

3. Experiments and results

The material used in this study was medium carbon steel S35C. Its chemical composition and the configuration of the specimens are shown in Table 1 and Fig.4. Strain gauges (30mm) were attached to the specimen polished (emery paper #1500) after the heat

Table 1 Chemical composition of the specimen

C	Si	Mn	P	S	Ni	Cr	Cu
0.34	0.24	0.76	0.03	0.03	0.04	0.13	0.09

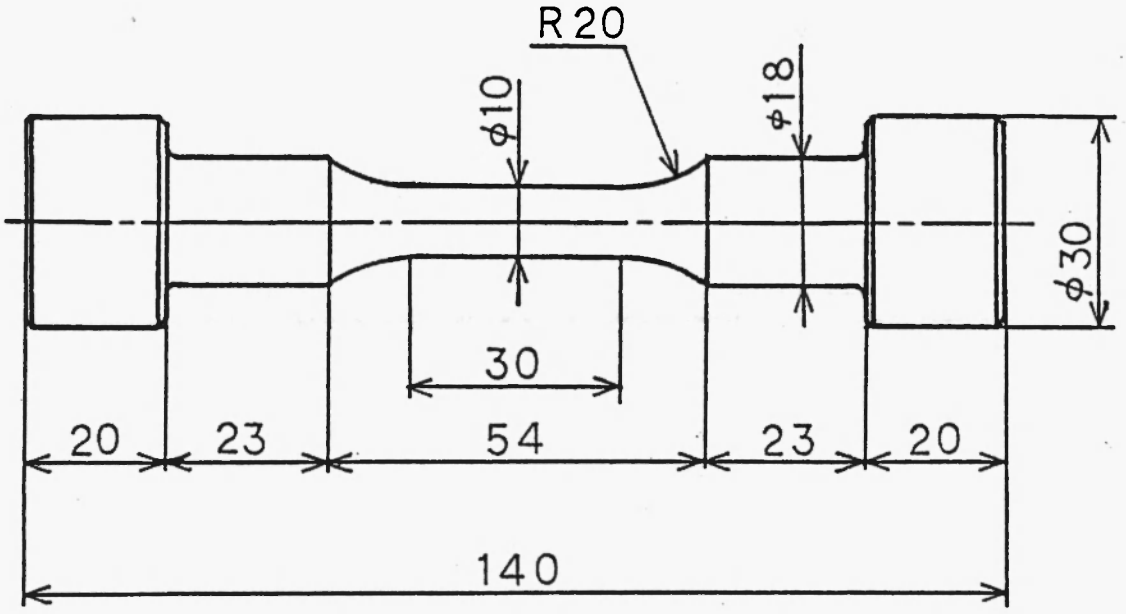

Fig.4 Configuration of test specimen

treatment. Fatigue tests were carried out at 20Hz under completely reversed tension-compression (stress ratio R=-1). Internal stress, effective stress, relaxation strain, and plastic strain amplitude, which are abbreviated as σ_i, σ_{eff}, ε_r and $\Delta\varepsilon_p$ respectively, were intermittenly monitored only at the maximum and the minimum level of the applied stresses.

Tests of six types were made:

(1) Fatigue tests under constant stress amplitude at a stress below and above the fatigue limit,
(2) Removal of surface layers by mechanical polishing during fatigue tests under constant stress amplitude at a stress above the fatigue limit,
(3) Fatigue tests under stepwise increasing stress amplitude,
(4) Fatigue tests under constant effective stress,
(5) Fatigue damage evaluations using a new cumulative damage rule,
(6) Observations of transient behaviour of σ_i, σ_{eff} and $\Delta\varepsilon_p$ under two-step cycling.

3.1 Fatigue Tests under Constant Stress Amplitudes

Four specimens were tested under constant stress amplitudes in order to know the behaviour of σ_i, σ_{eff} and $\Delta\varepsilon_p$ with the progress of fatigue. Two were tested above the fatigue limit at 207 and 196 MPa respectively (fatigue limit σ_w = 187MPa), and the remaining two at 186 and 182 MPa below the fatigue limit. The results are shown in Figs.5 to 7.

Two specimens fatigued at the overstressed level fractured at 7×10^4 cycles (207MPa) and 1×10^5 cycles (196MPa) respectively, while the other specimens fatigued at understressed level (186 and 182 MPa) endured up to 1×10^7 cycles. σ_i had a tendency to increase while σ_{eff} decreased in every case and

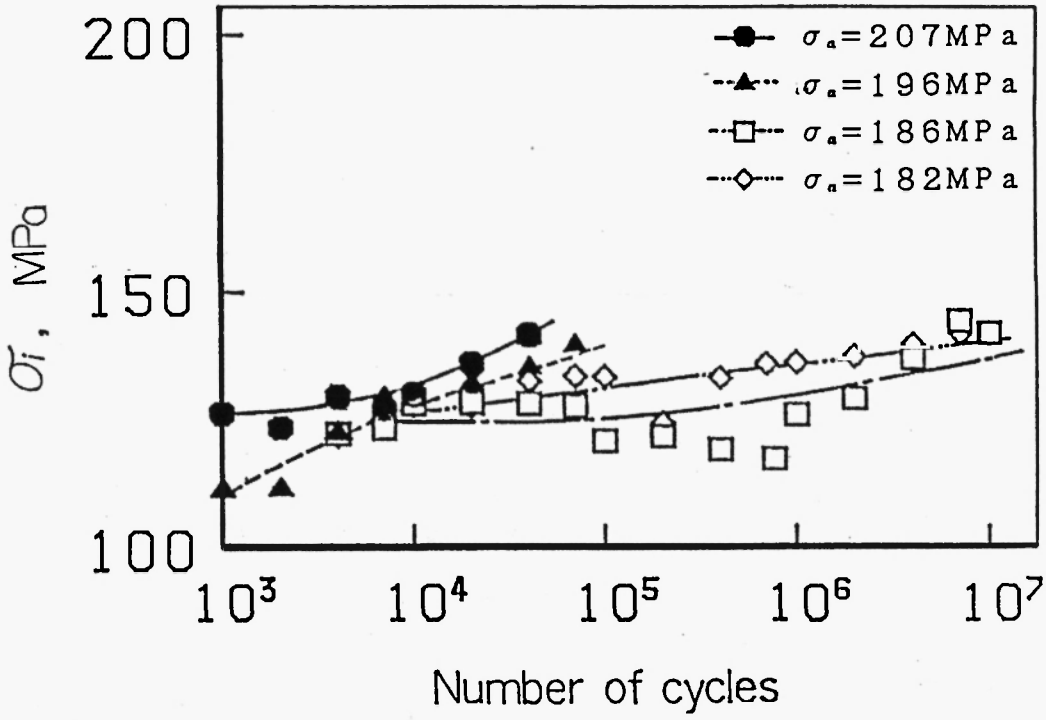

Fig.5 Change in internal stress during fatigue under constant stress amplitudes σ_a=207, 196, 186 and 182MPa

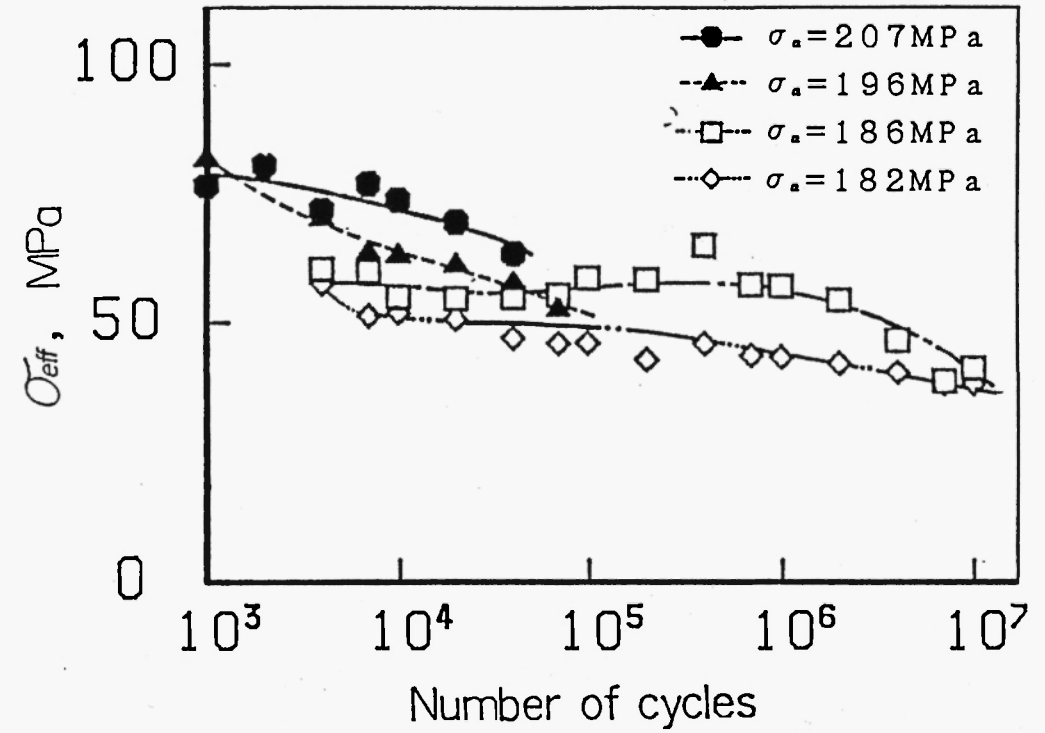

Fig.6 Change in effective stress during fatigue under constant stress amplitudes σ_a=207, 196, 186 and 182MPa

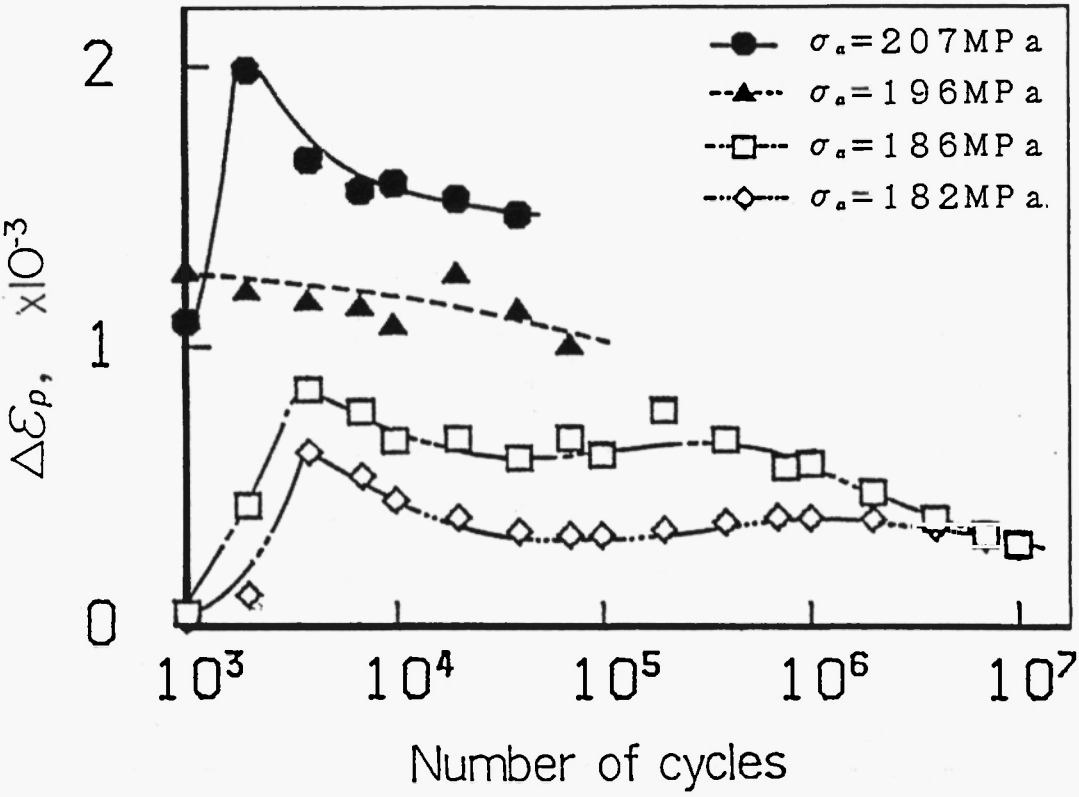

Fig.7 Change in plastic strain amplitude during fatigue under constant stress amplitudes σ_a=207, 196, 186 and 182MPa

the value of σ_{eff} was greater in overstressed cases than in understressed cases, except for early stages of life where fatigue deformation was not stable, and also except for the final stages of life where cracks might be propagating and these factors might no longer be meaningful.

3.2 Removal of Surface Layers during Fatigue Test

In order to detect the fatigue resistivity of the material, at the 10% overstressed level(206MPa) above the fatigue limit, the specimen was cycled with periodic mechanical removal of its surface in 50 μm thickness at intervals of 1×10^5 cycles until $\Delta\varepsilon_p$

became less than 300×10^{-6}; thereafter no polishing was applied to the specimen.

At 2.2×10^{6} cycles after the 22nd polishing, $\Delta\varepsilon_p$ reached less than 300×10^{-6} and the specimen, which no more polishing was given to, endured up to 1×10^{7} cycles at the same stress level(206MPa) without fracture, as shown in Figs.8 and 9. The same kind of test carried out at an 15% overstressed level(215MPa), above the fatigue limit showed that $\Delta\varepsilon_p$ did not reach 300×10^{-6}, and the specimen fractured in the end.

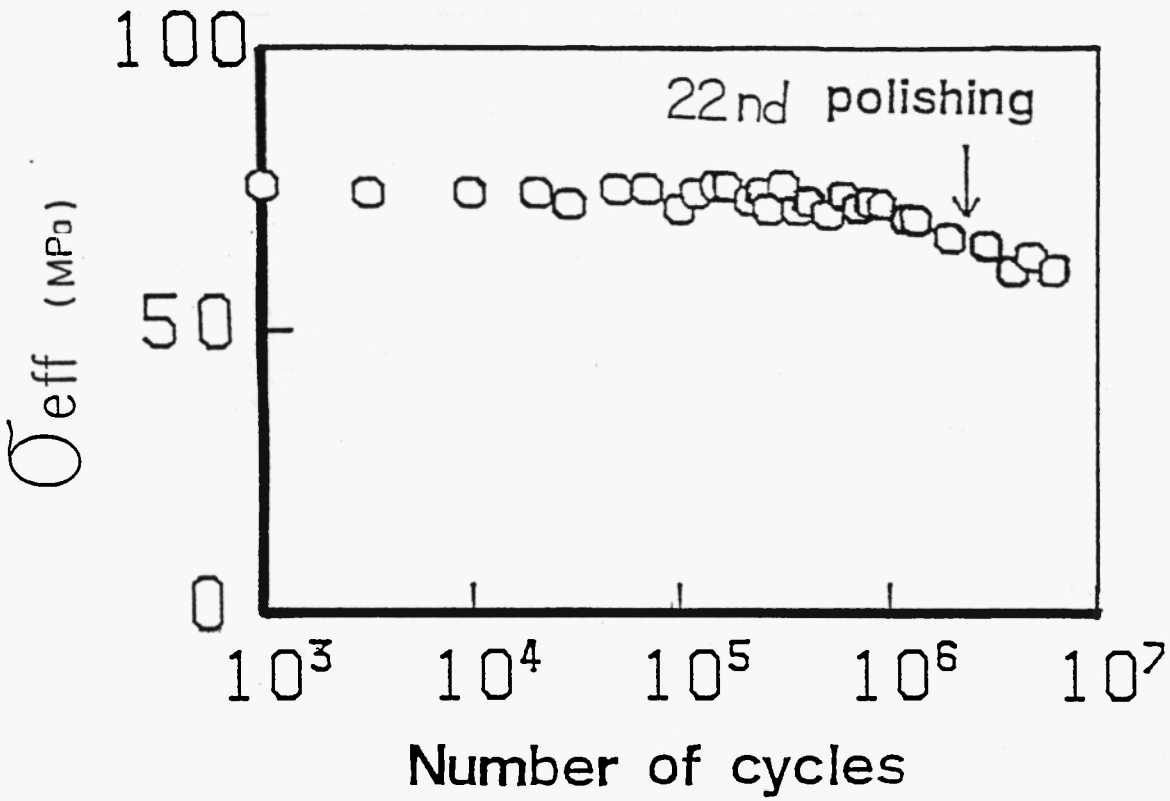

Fig.8 Change in effective stress during fatigue under constant stress amplitude σ_a=206MPa by removal of surface layers

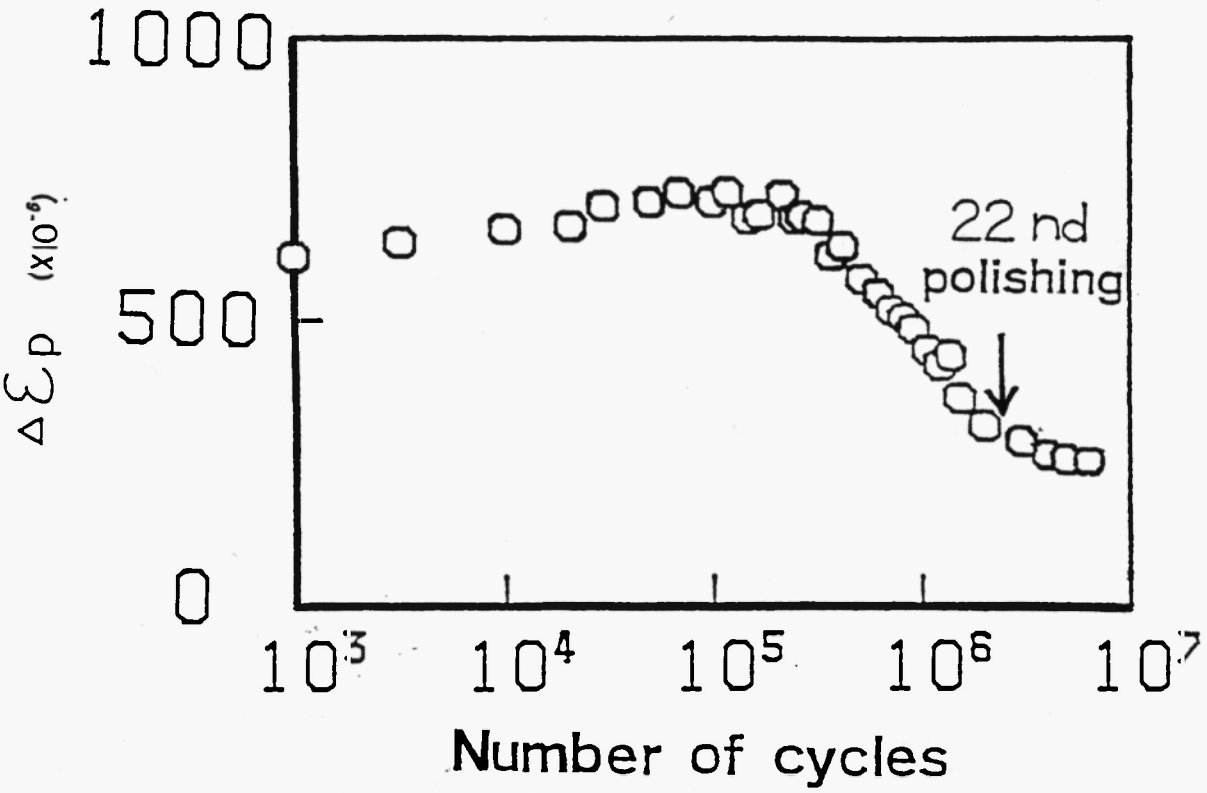

Fig.9 Change in plastic strain amplitude during fatigue under constant stress amplitude σ_a=206MPa by removal of surface layers

3.3 Fatigue Test under Stepwise Increasing Stress Amplitude

Internal stress was measured under coaxing effect[10], starting at a stress level 4MPa lower(183MPa) than the fatigue limit with an increment of 4.9MPa after each 1x10^7 cycles. The internal stress, shown in Fig.10, was observed to increase as the period became longer, tending closer to the applied stress than at earlier periods.

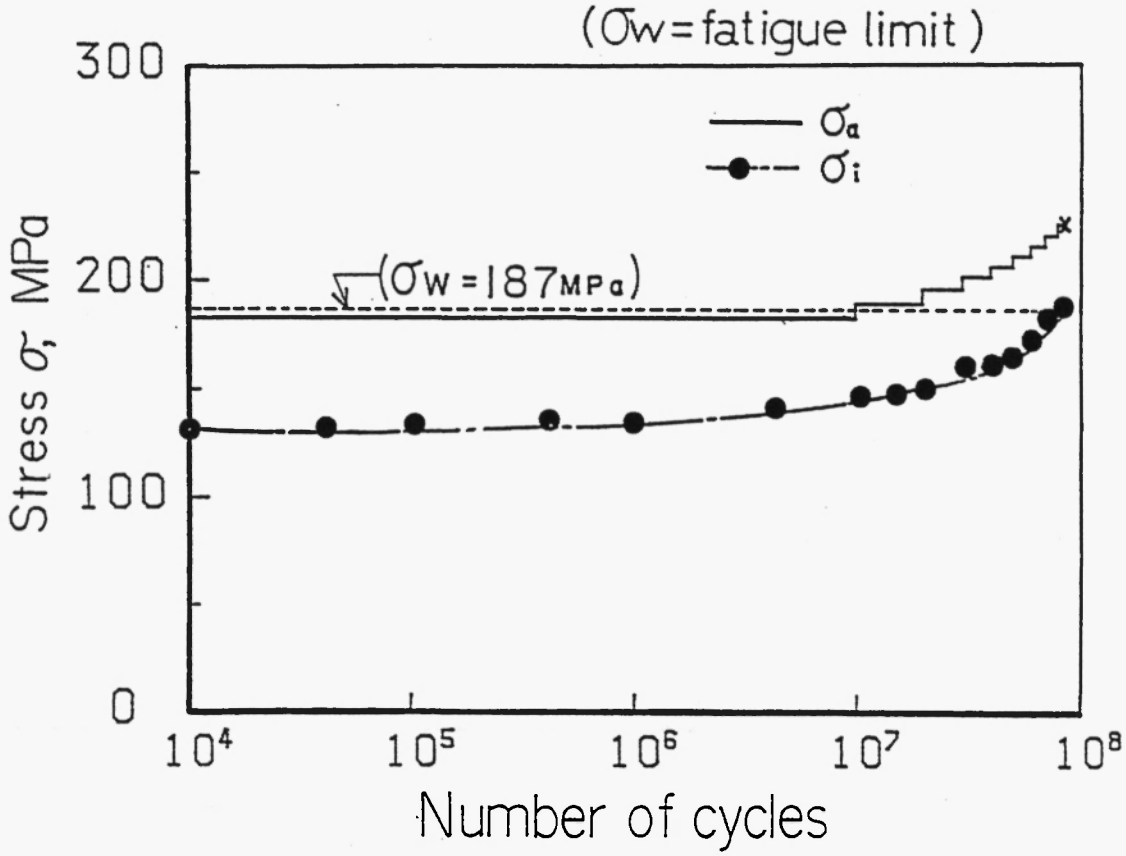

Fig.10 Change in internal stress σ_i and applied stress amplitude σ_a during fatigue under stepwise increasing stress amplitude

3.4 Fatigue Tests under Constant Effective Stresses

These tests were conducted by controlling applied stress to hold the effective stress constant with the aid of frequent monitoring of the effective stress during stress cycling. The tests were carried out in two stages.

First, a virgin specimen and a previously fatigued one (1×10^7 cycles at 182MPa, a little below the fatigue limit, and then its surface polished) were tested at the same effective stress level, resulting in

the same period of fatigue life as shown in Fig.11. Successively, fatigue tests were made at various effective stress levels, and Fig.12 was obtained. The "S-N like" curve line (ES-N curve) in the figure had also a fatigue limit at 61MPa.

3.5 Fatigue damage evaluations using a new cumulative damage rule

Fatigue tests under constant stress amplitude and under manifold multiple repeated stress in two stress

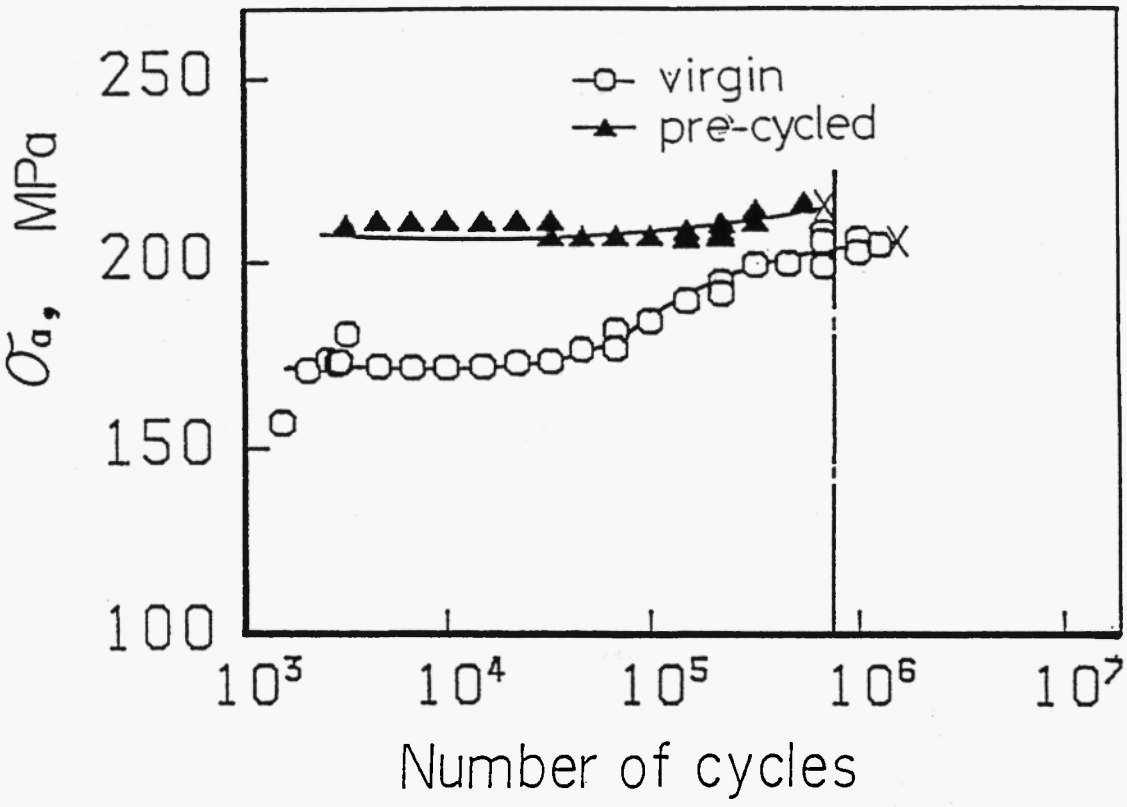

Fig.11 Change in applied stress amplitude σ_a during fatigue under constant effective stress at 69 MPa, annealed (virgin) specimen and pre-cycled (σ_a=186MPa, 1x10^7 cycles) one being used.

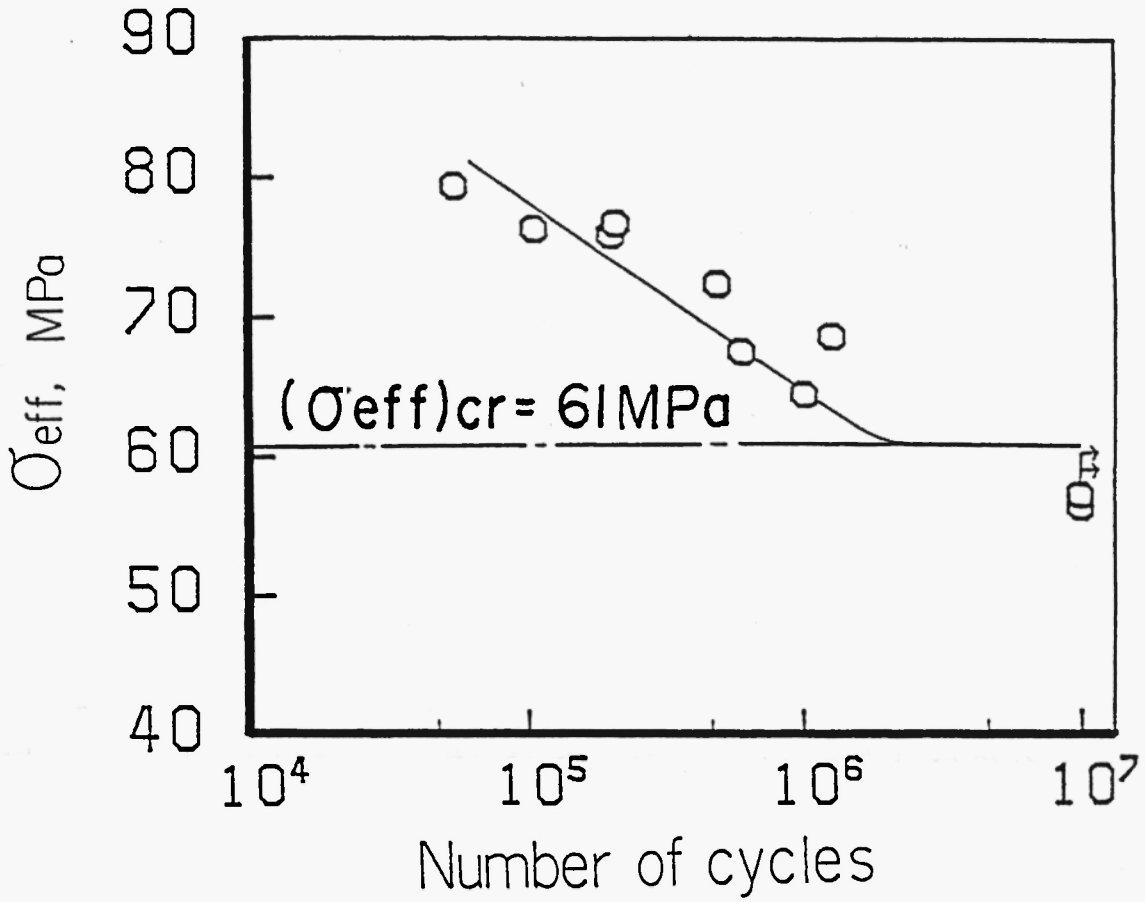

Fig.12 ES-N curve

levels were made to measure effective stress in order to evaluate fatigue damage in a manner similar to Palmgren-Miner's. Experimental results and accumulated damage evaluated according to Miner's rule using effective stress instead of applied stress, named ES-Miner's rule, are shown in Table 2 and Figs.13 and 14, with comparison to Miner's evaluations.

Regardless of the specimen's fracture or not, Miner's value $\sum (n_i/N_i)_c$ exceeded unity. However, in the case of fracture, ES-Miner's value $\sum (n_i/N_i)_{es}$ kept increasing in the range less than unity, while in

Table 2 Results of fatigue test under constant stress amplitude and manifold multiple repeated stress in two stress levels.

Specimen number	σ_1 (MPa)	σ_2 (MPa)	n_1	n_2	N_f	Cumulative damage value			
						based on Miner's rule			based on ES-Miner's rule
						n_1/N_1	n_2/N_2	$\Sigma (n_i/N_i)_M$	$\Sigma (n_i/N_i)_{ES}$
1	182	–	–	–	non-fractured	0	–	0	0.004
2	182	–	–	–	non-fractured	0	–	0	0.261
3	192	–	–	–	non-fractured	>16.669	–	>16.669	0.946
4	192	–	–	–	4.676×10^5	0.779	–	0.779	0.685
5	197	–	–	–	2.944×10^5	1.052	–	1.052	0.396
6	202	–	–	–	3.126×10^5	2.396	–	2.396	0.949
7	202	–	–	–	9.447×10^4	0.724	–	0.724	1.044
8	207	–	–	–	7.912×10^4	1.300	–	1.300	1.268
9	206	98	200	9800	non-fractured	>3.894	0	>3.894	0.266
10	206	181	200	9800	non-fractured	>4.178	0	>4.178	0.030
11	206	157	200	9800	non-fractured	>3.041	0	>3.041	0.214
11'	206	–	–	–	1.102×10^7	10.630	–	10.630	0.719
12	206	191	200	800	6.518×10^5	1.840	0.746	2.586	0.730
13	206	191	500	500	6.631×10^5	4.678	0.474	5.152	0.538

[Notes] Specimens, No.1-8, were fatigued under constant stress amplitude, and the other specimens No.9-13, were fatigued under manifold multiple repeated stress in two levels.
No.11' was fatigued under constant stress amplitude, σ_1, after fatigue test of No.11 in order to check ES-Miner's value getting closer to unity when the specimen No.11 was fractured.

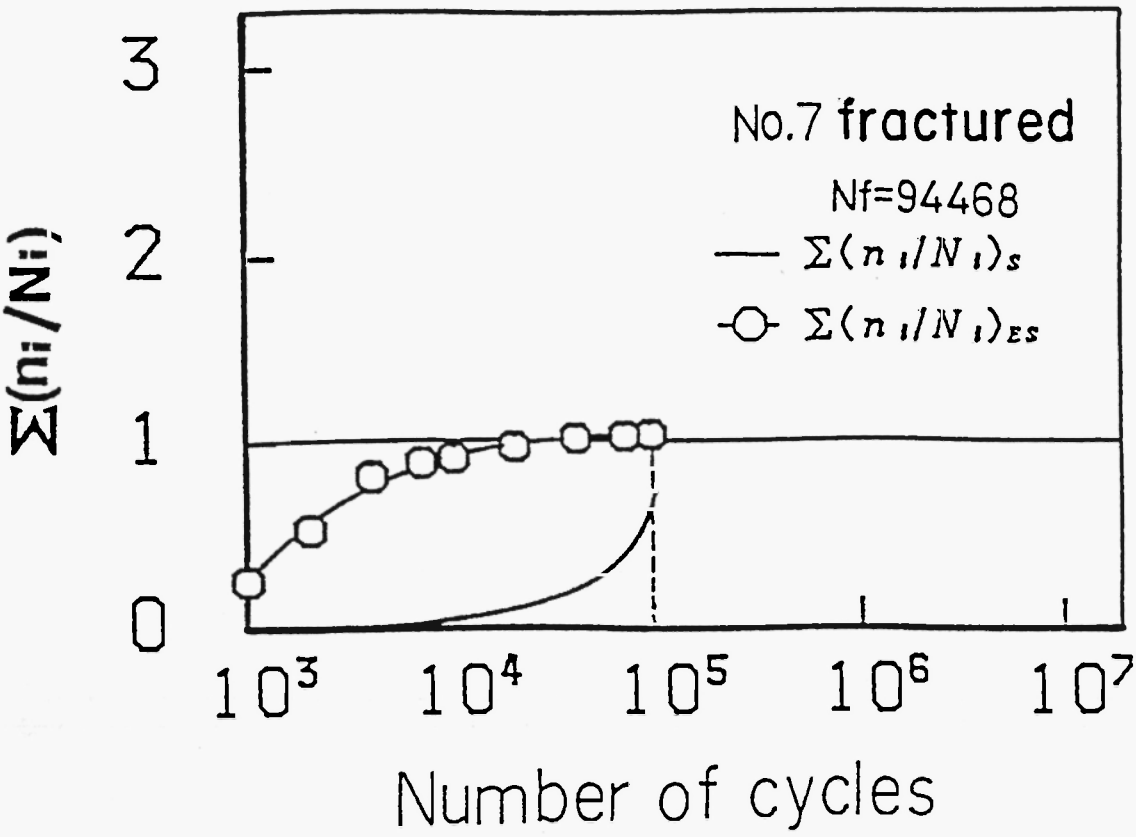

Fig.13 Change in values of cumulative damage (or cumulative cycle ratio) estimated by two methods, Miner's method and ES-Miner's method, during fatigue of specimen No.7 (fractured).

the case of non-fracture, $\Sigma (n_i/N_i)_{es}$ stopped increasing in the latter period of the fatigue process

3.6 Observation of transient behaviour of σ_i, σ_{eff} and $\Delta\varepsilon_p$ under two-step cycling

Six two-step cycling tests under the condition shown in Table 3 were made in order to reveal the transient behaviour of σ_i, σ_{eff} and $\Delta\varepsilon_p$ under stepwise stress fluctuation with the help of the "Elastic-Range Detection Test" (See Appendix B).

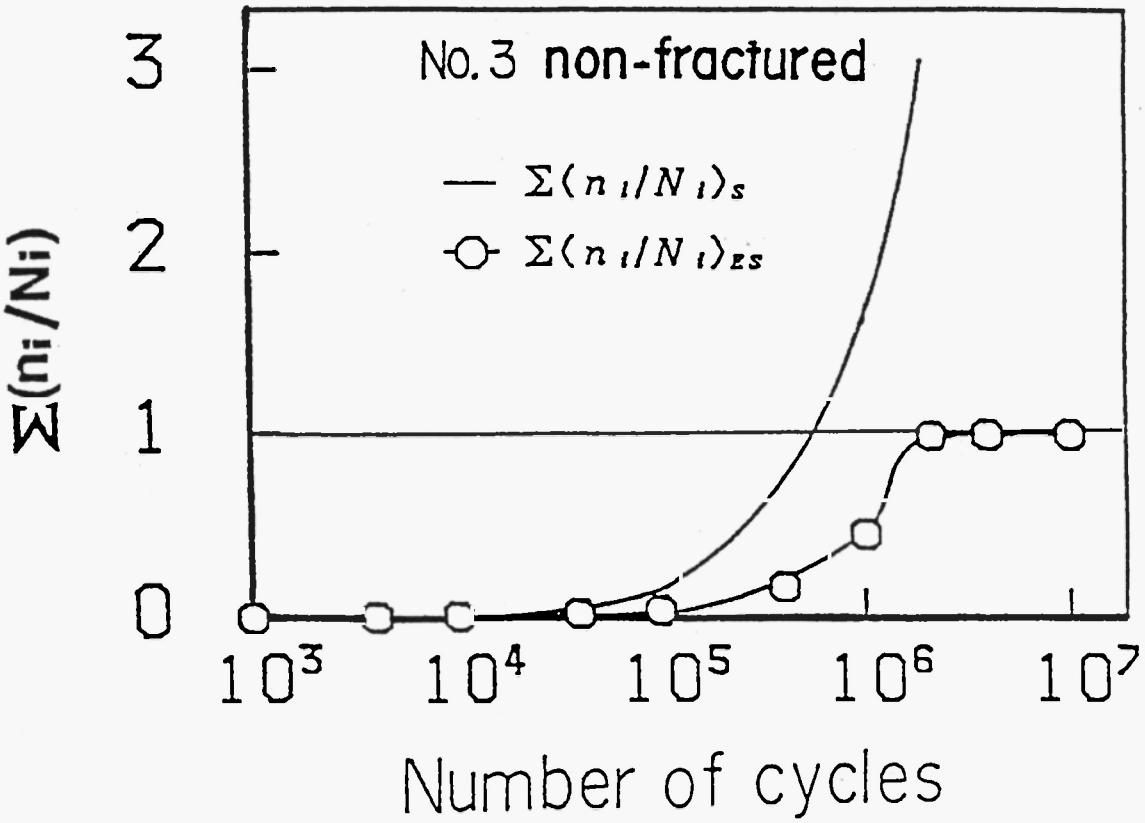

Fig.14 Change in values of cumulative damage (or cumulative cycle ratio) estimated by two methods, Miner's method and ES-Miner's method, during fatigue of specimen No.3 (non-fractured).

Since the specimens used here were previously fatigued ones ($1x10^7$ cycles at 182MPa, a little below the fatigue limit, and then their surfaces were polished), their fatigue deformation was stable and transient behaviour was observable.

Results are shown in Figs.15 and 16. Effective stress temporarily increases while internal stress decreases just after stress fluctuations, and then they converge into a certain stress level corresponding to an applied stress of the second stage; of less than several thousand cycles in every case.

Table 3 Experimental conditions of the two-step cycling test

	Stress level		Block size (cycles)	
	σ_1 (MPa)	σ_2 (MPa)	N_1	N_2
1	182	200	6,000	5,000
2	199	216	〃	〃
3	198	222	〃	〃
4	208	219	〃	〃
5	207	226	〃	〃
6	226	213	〃	〃
7	226	210	〃	〃
8	223	204	〃	〃
9	202	183	〃	〃

[Notes] No,1-5:Two-step increasing test
No,6-9:Two-step decreasing test

4. Discussion

4.1 The fatigue limit

A cyclically stressed material increases its resistivity to stresses causing fatigue deformation as shown in Figs.7 and 9. This behavior of the material is detectable through measurements of internal stresses during the fatigue process. The transient behaviours shown in Section 3.6 mean that the magnitude of the internal stress is dependent on the loading history of the material. Internal stress can thus be understood

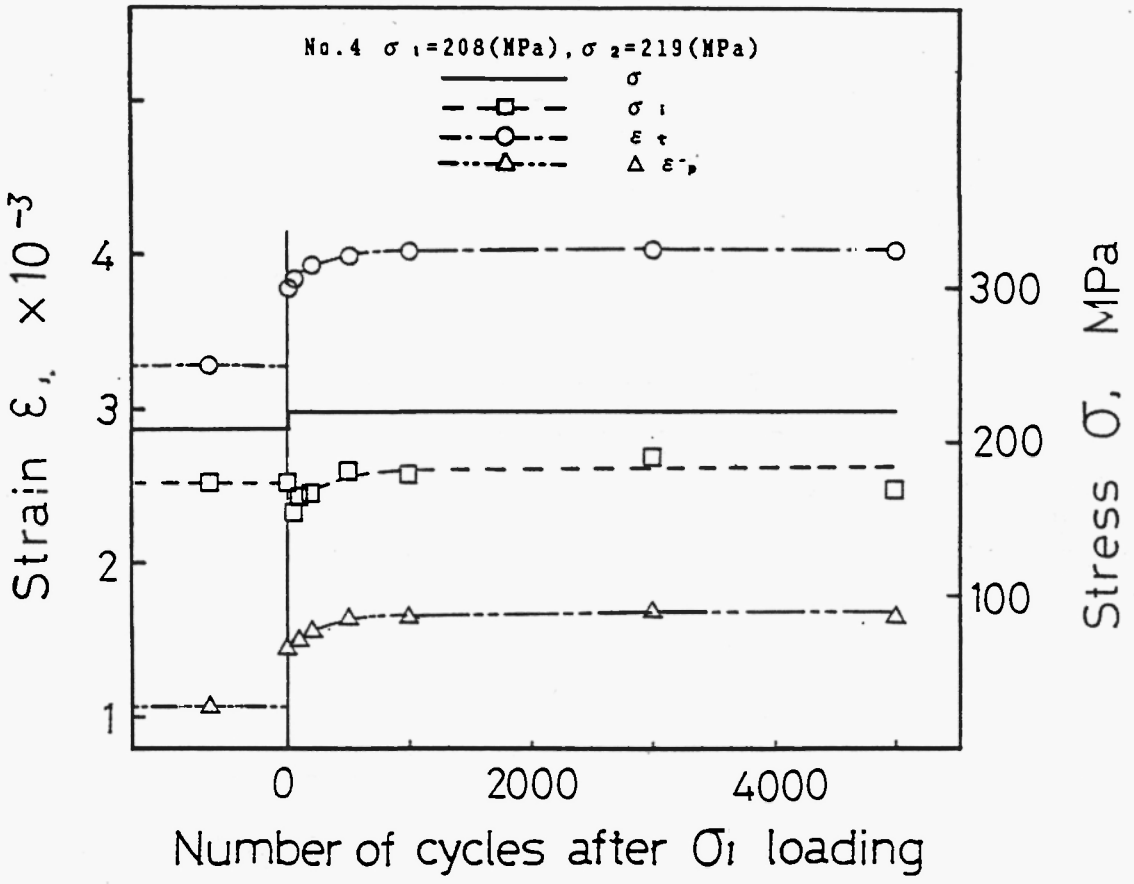

Fig.15 Change in values of σ_i, σ_{eff} and $\Delta\varepsilon_p$ under two-step increasing test at a stress of the 1st stage σ_1 = 208MPa and σ_2 = 219MPa

to be representative of fatigue resistivity of the material at that particular moment.

On the other hand, effective stress is responsible for fatigue deformation, hence the fatigue damage increment to the material. The results shown in Fig.11 suggested that effective stress alone might be responsible for fatigue damage. Moreover, a fraction of the effective stress above the limit of 61MPa in Fig.12 is responsible for fatigue damage as

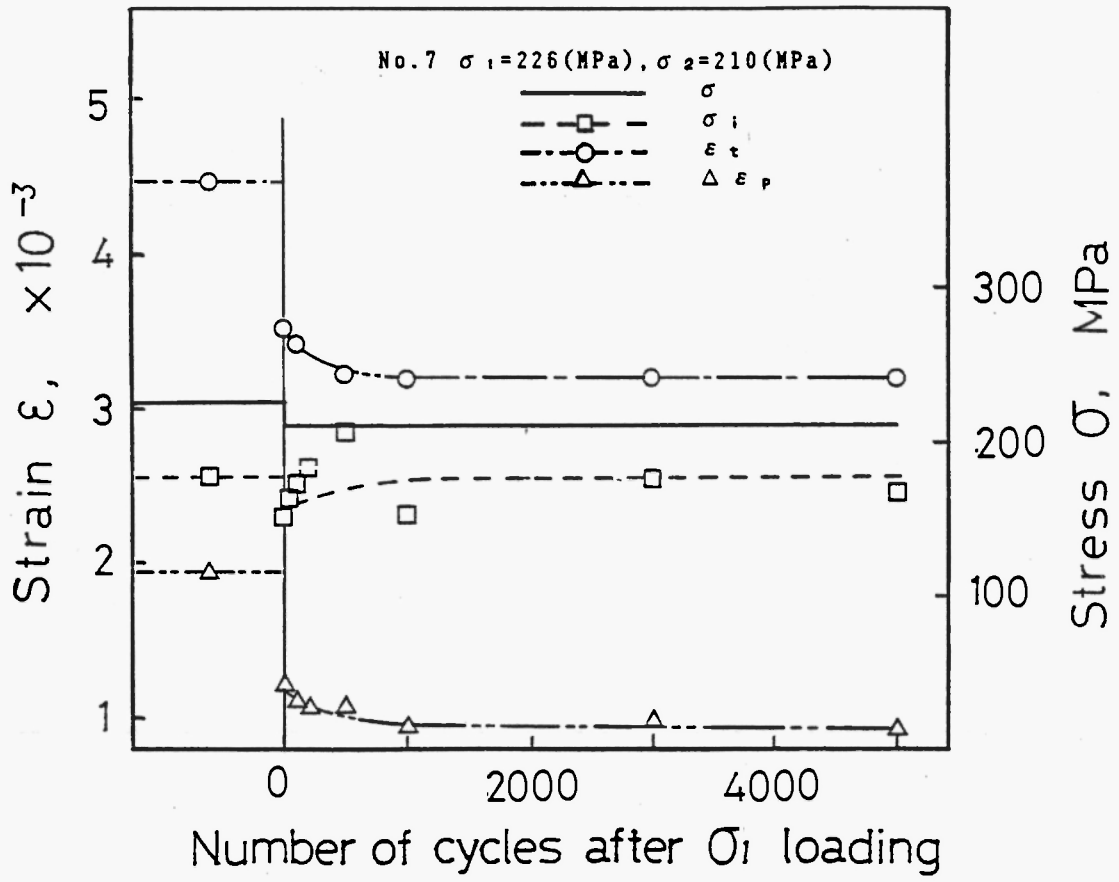

Fig.16 Change in values of σ_i, σ_{eff} and $\Delta\varepsilon_p$ under two-step decreasing test at a stress of the 1st stage σ_1 = 226MPa and σ_2 = 210MPa

illustrated in Fig.6, and the rest of the effective stress would give no fatigue damage to the material, that is, only to-and-fro motion of dislocations in the material.

The experimental result in Section 3.2, where a material shows a fatigue resistivity increase if its surface layer is occasionally removed, means that "fatigue damage" under these circumstances is accumulated at the surface in the form of surface flaws

such as persistent slip bands, intrusions, or extrusions.

A material, when fatigue-cycled, reacts in two competing behaviours:

The material suffers damage in the form of surface flaw due to effective stress. The increment of the damage corresponds to the excess of effective stress above a critical value. On the other hand, the material is strengthened to endure further stressing in proportion to the internal stress increase through the dislocation reaction, or strain ageing of the material.

When the material damage and the material strengthening effects are in balance, a fatigue limit is reached depending on the stress history.

4.2 New cumulative damage criterion

This new cumulative damage rule shown in Section 3.5, ES-Miner's rule, may give a better estimation of damage than that by Miner's rule in all cases. The superiority of this rule is that it indicates a trend toward saturation of accumulated damage, which is not found in other damage criteria such as Miner's or Erdogan's, through decrease of effective stress during fatigue process. This is because fatigue resistivity or fatigue hardening, which reflects stress history, is evaluated in this method in terms of an increase of internal stress.

Additionally, stress fluctuations would give more fatigue damage to the material than in the absence of without stress fluctuations. The effective stress temporarily increases just after stress fluctuation, even if the applied stress shifts up or down, as shown in Section 3.6. Hence surplus fatigue damage would be accumulated on the material in a transition period of the stress-strain behaviour[11].

This method of damage estimation may be applied also in the case of practical fatigue under varying stress conditions if data on the actual behaviour of effective stress throughout fatigue process is obtainable.

5. Conclusions

A new approach was applied to fatigue studies, which enabled applied stress to be divided into two parts: internal stress and effective stress. Several experimental results were analyzed and discussed on the basis of these concepts, leading to the following conclusions:

(1) Fatigue damage is generated by effective stress causing fatigue deformation and is accumulated on the surface of cyclically stressed material in the form of surface roughness, by the removal of which the material becomes free from damage.

(2) Fluctuations in the applied stress give more fatigue damage to the material than in the absence of stress fluctuation.

(3) A material shows increasing "fatigue resistivity" under cyclically stressed conditions, which can be monitored in terms of internal stress.

(4) The increment of fatigue damage can be evaluated in terms of the magnitude of effective stress.

(5) Fatigue mechanism is discussed as a competition between two mechanisms : damage due to effective stress and strengthening as monitored in terms of internal stress. The fatigue limit may be regarded as the case of their balance.

(6) A new cumulative damage rule is proposed and discussed.

References

(1) J.C.Levy and G.M.Sinclair: "An Investigation of Strain Aging in Fatigue," Proc. ASTM, 55(1955),866.

(2) S.Seike, S.Kitaoka et.al.: "Understressing Effect in Eutectoid Steel at -60 C" (No original English title, translated by contributor) Trans. of JSME, 40(1974),609. (in Japanese)

(3) A.Yoshikawa and T.Sugeno: "Factors Responsible for the Sharp Fatigue Limit in Iron and Steel", Trans.Met.Soc.,AIME, 233(1965),1314.

(4) T.Nakagawa and Y.Ikai: "Strain Ageing and Fatigue Limit in Carbon Steel", Fatigue Eng.Mater.Struct., 2(1980),13.

(5) E.Orowan: "Problems of Plastic Gliding", Proc.Phys.Soc., 52(1940),8.

(6) A.Seeger: "Theorie der Kristallplastizitat III.Die Temperatur und Geshwindigkeitsabhangigkeit der Kristallplastizitat" Z.Naturforschg.,9a(1954),870.

(7) J.C.M.Li: "Dislocation Dynamics in Deformation and Recovery", Can.J.Phys.,45(1967),493.

(8) S.R.MacEwen, O.A.Kupcis et.al.: "An Investigation of an Incremental Unloading Technique for Estimating Internal Stresses", Scripta Met.,3(1969),441.

(9) J.Polak, M.Klesnil et.al.: "Stress Dip Technique for Effective Stress Determination in Cyclic Straining", Scr.Met., 13(1979),847.

(10) G.M.Sinclair: "An Investigation of the Coaxing Effect in Fatigue of Metals", Proc. ASTM,52(1952),743.

(11) C.Iwasaki and Y.Ikai: "Fatigue Failure at Stress below Fatigue Limit", Fatigue Fract. Engng Mater. Struct., 9(1986),117.

(12) W.G.Johnston and J.J.Gilman: "Dislocation Velocities, Dislocation Densities, and Plastic Flow in Lithium Fluoride Crystals", J. Appl. Phys., 30(1959),129.

(13) M.Mughrabi: "Dislocation Wall and Cell Structures and Long Range Internal Stresses in Deformed Metal Crystals", Acta Met.,31(1983),1367.

Appendix A

Origin of internal stress and effective stress

A theoretical relationship between the plastic strain rate $\dot{\varepsilon}_p$, the average dislocation velocity v and mobile dislocation density ρ_m was proposed by E.Orowan[5] in the form

$$\dot{\varepsilon}_p = \alpha b \rho_m v \qquad (A1),$$

where α is a geometric factor and b is the absolute value of Burger's vector. On the other hand, an empirical relationship between v and the shear stress acting on a dislocation τ_{eff} was found by W.G.Johnston and J.J.Gilman[12] in the form

$$v = B \cdot \tau_{eff}^{m} \qquad (A2),$$

where B and m are constants at a given temperature. Combining these two equations, we obtain a relationship between $\dot{\varepsilon}_p$, ρ_m and τ_{eff} in the form

$$\dot{\varepsilon}_p = \alpha b B \rho_m \qquad (A3).$$

Since a moving dislocation encounters resistive stress σ_i from other dislocations through long-range elastic interactions, the applied stress σ_a does not fully act on the dislocation but the net stress σ_{eff}, which is equivalent to $\sigma_a - \sigma_i$, acts on it. σ_i is called internal stress and σ_{eff} effective stress.

The origin of internal stress[11] is a long-range elastic interaction between dislocations which have a tendency to condense to form dislocation cell structures, and internal stress is concentrated at the

cell boundaries The latter is supported by direct TEM observations by H.Mughrabi[13].

Appendix B

Elastic-Range detection Test.

The "Elastic-Range detection test" is used to measure the effective stress using the stress-strain hysteresis relationship for a low-carbon steel, which is characterized as having the elastic range. This method enables us to obtain the effective stress in a stress-strain transition period, where the "strain-transient dip test" cannot be applied.

Since no effective stress acts on the dislocations in the elastic range region, strain increases linearly with applied stress. The elastic range is detected as a straight line section of the stress-strain hysteresis with a regression analysis of the 1st order, and threshold values of the elastic range (A, B, D and E shown in Fig.2) are obtainable.

Effective stress is given by the relationship found in preliminary experiment between σ_{eff} and applied stress σ_a in the form

$$\sigma_{eff} = \frac{\sigma_C - \sigma_D}{\sigma_C - \sigma_B} (\sigma_a - \sigma_B) \quad (B1),$$

where σ_B is the stress level at point B, σ_C at C, σ_D at D respectively.